


Thermodynamics of enzyme-catalyzed esterifications: II. Levulinic acid esterification with short-chain alcohols

Emrah Altuntepe¹ · Vladimir N. Emel'yanenko² · Maximilian Forster-Rotgers¹ ·
Gabriele Sadowski¹ · Sergey P. Verevkin³ · Christoph Held¹ 

Received: 5 June 2017 / Revised: 4 August 2017 / Accepted: 9 August 2017 / Published online: 14 September 2017
© Springer-Verlag GmbH Germany 2017

Abstract Levulinic acid was esterified with methanol, ethanol, and 1-butanol with the final goal to predict the maximum yield of these equilibrium-limited reactions as function of medium composition. In a first step, standard reaction data (standard Gibbs energy of reaction $\Delta^R g^0$) were determined from experimental formation properties. Unexpectedly, these $\Delta^R g^0$ values strongly deviated from data obtained with classical group contribution methods that are typically used if experimental standard data is not available. In a second step, reaction equilibrium concentrations obtained from esterification catalyzed by Novozym 435 at 323.15 K were measured, and the corresponding activity coefficients of the reacting agents were predicted with perturbed-chain statistical associating fluid theory (PC-SAFT). The so-obtained thermodynamic activities were used to determine $\Delta^R g^0$ at 323.15 K. These results could be used to cross-validate $\Delta^R g^0$ from experimental formation data. In a third step, reaction-equilibrium experiments showed that equilibrium position of the reactions under consideration

depends strongly on the concentration of water and on the ratio of levulinic acid: alcohol in the initial reaction mixtures. The maximum yield of the esters was calculated using $\Delta^R g^0$ data from this work and activity coefficients of the reacting agents predicted with PC-SAFT for varying feed composition of the reaction mixtures. The use of the new $\Delta^R g^0$ data combined with PC-SAFT allowed good agreement to the measured yields, while predictions based on $\Delta^R g^0$ values obtained with group contribution methods showed high deviations to experimental yields.

Keywords PC-SAFT · Novozym 435 · Water activity · Reaction equilibrium prediction · Activity coefficient · Vapor pressure · Enthalpy · Thermochemistry

Introduction

The depletion of fossil resources and emerging environmental issues lead to massive efforts that are directed to identify attractive renewable energy and material resources. Within this context, biomass is recognized as resource for sustainable production of chemicals and fuels. (Alonso et al. 2010; Démolis et al. 2014; Weingarten et al. 2011; Zhang et al. 2012) Significant attention has therefore addressed renewable replacements for petroleum-based resources, because utilization of biomass represents a carbon-neutral and sustainable route for synthesis (Schwartz et al. 2014). Nevertheless, the practical conversion of biomass towards desired fuels and chemicals is still an enormous challenge for industry (Demma Carà et al. 2014; Kamm et al. 2000). Concepts are developed that integrate various production pathways in one process in order to overcome technical barriers and to become more competitive compared to classical fossil-based synthesis routes (Zhang 2008).

Electronic supplementary material The online version of this article (<https://doi.org/10.1007/s00253-017-8481-4>) contains supplementary material, which is available to authorized users.

✉ Christoph Held
christoph.held@bci.tu-dortmund.de

Sergey P. Verevkin
sergey.verevkin@uni-rostock.de

¹ Laboratory of Thermodynamics, Department of Biochemical and Chemical Engineering, Technische Universität Dortmund, Emil-Figge-Str. 70, 44227 Dortmund, Germany

² Chemical Department, Samara State Technical University, Molodogvardeyskaya 244, Samara, Russia 443100

³ Department of Physical Chemistry and Department of Science and Technology of Life, Light and Matter, University of Rostock, Dr-Lorenz-Weg 2, D-18059 Rostock, Germany

Various components obtained from biomass have been reported to have huge potential for serving as platform chemicals for chemical pathways and (bio-) transformations (Alonso et al. 2010; Kobayashi and Fukuoka 2013; Serrano-Ruiz et al. 2011). Levulinic acid (LA) belongs to this class of compounds. It has been reported as one of the most promising biomass-derived platform chemicals (Climent et al. 2014; Dautzenberg et al. 2011; Pileidis and Titirici 2016; Wery and Petersen 2004; Wu et al. 2016). The bio-based synthesis of LA is discussed in literature extensively and will not be described here. In a published review from Pileidis and Titirici, synthesis of LA is discussed, including catalysis (homogeneous and heterogeneous catalysis) and the kind of starting material like for example furfural, 5-hydroxymethylfurfural, different sugars, lignocellulosic materials, and agricultural waste (Pileidis and Titirici 2016). LA contains a ketone group and a carboxylic acid group in its structure. These make LA to a very versatile building block for the synthesis of various chemicals, such as gamma-valerolactone, alkyl levulinates, 2-methyltetrahydrofuran, and acrylic acid (Bozell et al. 2000; Démolis et al. 2014; Isikgor and Becer 2015; Pileidis and Titirici 2016; Timokhin et al. 1999; Zhang et al. 2012).

Especially the alkyl levulinates have been recognized as very interesting LA derivatives due to their specific physicochemical properties and their range of applications (Leibig et al. 2011; Olson et al. 2001; Wery and Petersen 2004; Zhang et al. 2012). The alkyl levulinates methyl-, ethyl-, and butyl levulinates are short-chain esters that are applicable in fields like flavorings and in fragrance industry (Bart et al. 1994; Lomba et al. 2013; Olson 2001). Besides, the esters of LA gained much interest as fuel additives. This is caused by the properties of the short-chain esters, such as non-toxicity, high lubricity, and flashpoint stability. (Christensen et al. 2011; Chung et al. 2015; Hayes 2009; Lomba et al. 2013) Further, these esters are discussed to be promising starting materials for various (bio-) chemical reactions. (Démolis et al. 2014; Olson 2001; Pileidis and Titirici 2016) Demolis et al. reviewed the synthesis and the application of alkyl esters (Démolis et al. 2014). In the literature, acid-catalyzed synthesis of esters starting from LA or furfuryl alcohol or carbohydrates in alcohols are suggested. Investigations showed that very different yields were obtained by using different reactants, and homogeneous and heterogeneous catalysis was studied and reviewed (Démolis et al. 2014; Pileidis and Titirici 2016).

In this work, the lipase-catalyzed esterification of LA in alcohol will be presented. Compared to chemical reaction routes, publications on enzyme-catalyzed synthesis are still scarce, although enzymatic synthesis provides several advantages in comparison to chemical esterification such as mild reaction conditions, lower energy requirement, and

easier catalyst removal and reusability, cheapness, and good stability even in non-aqueous media (Lilly 1994; Petersson et al. 2005; Turner 1995). In this work, the enzyme *Candida antarctica* lipase B immobilized on acrylic resin (Novozym 435) was used. It was reported that this enzyme catalyzes the esterification of LA with ethanol (EtOH) or 1-butanol (1-BuOH). (Lee et al. 2010; Yadav and Borkar 2008) Lee et al. investigated the effect of several reaction conditions like enzyme amount, reaction time, temperature, and reactant ratio on the conversion of LA in solvent-free system (Lee et al. 2010). The dependence of conversion of enzyme amount suggests that not all of their data is equilibrium data. Besides conversion, Yadav et al. suggested a reaction mechanism and developed a kinetic model for the esterification of LA with 1-BuOH catalyzed by three different immobilized lipases in tetra-butyl methyl ether as solvent (Yadav and Borkar 2008). Although all these works let assume that a significant amount of work on kinetics of LA esterification exists in the literature, studies on thermochemistry and equilibrium thermodynamics of these reactions are still scarce. Bart et al. (Bart et al. 1994) have performed according experiments on esterification of LA with 1-BuOH catalyzed by sulphuric acid, and a kinetic model as well as equilibrium constants and reaction enthalpies were determined. However, these data neglect thermodynamic non-idealities due to deviations from ideal-mixture behavior by assuming activity coefficients of reacting agents to be one. Chung et al. used the kinetic model of Bart et al. in order to describe a reactive distillation system for the esterification of LA and 1-BuOH (Chung et al. 2015). This work is important and pioneering as it addresses purification concepts and unit operations for processes with LA esterification, which was accessed by thermodynamic modeling with NRTL (Chung et al. 2015).

In this work, the reaction equilibrium of the LA esterification with methanol, ethanol, and 1-butanol was investigated at 323.15 K. Novozym 435 was used as catalyst for the reactions. These reactions were studied under different reactant ratios and for different water concentrations in the initial reaction mixtures. In order to determine the thermodynamic equilibrium constant of the reactions, thermodynamic activities of the reacting agents were required. For this purpose, activity coefficients of the reacting agents were predicted by perturbed-chain statistical associating fluid theory (PC-SAFT) (Gross and Sadowski 2001; Gross and Sadowski 2002). In our previous work, PC-SAFT has been proved as successful model for the prediction of activity coefficients in multi-component reaction mixtures (Altuntepe et al. 2017a; Hoffmann et al. 2013; Riechert et al. 2015). In a final step, the obtained thermodynamic properties and equilibrium constants were used in order to predict conversions by iteratively solving the equations for reaction equilibrium.

Experiments and methods

Materials

Chemicals that have been used in this work are listed in Table S1. All chemicals were used as obtained without further purification. Lipase B from *Candida antarctica* was used as the immobilized form on acrylic resin (5 U mg⁻¹, supplier information). The immobilized lipase, expressed in *Aspergillus niger*, was purchased from Sigma-Aldrich Chemie GmbH. In the following, the immobilized enzyme will be denoted as Novozym 435. Deionized water from the Millipore system (Merck KGaA) was used. All abbreviations and symbols are listed in Table 1.

Reaction equilibrium experiments and analysis

The reactions investigated in this work take place in the liquid phase, while the enzyme is present as heterogeneous catalyst. The reaction experiments were carried out in two types of set-ups. Equilibrium experiments were performed in double-jacket 10-mL glass vessels with a reaction medium of 5 mL and in 1.5-mL closable plastic vessels with a reaction medium of 1 mL volume. The reaction temperature in the 10-mL glass vessels was adjusted to 323.15 K and controlled by F 25 thermostat from Julabo (Seelbach, Germany) with an accuracy of ± 0.03 K. The temperature in the closable 1.5-mL plastic vessels was controlled in the ThermoMixer® comfort with a 1.5-mL thermoblock (Eppendorf, Hamburg, Germany). The glass vessels were stirred with a speed of 800 rpm, and the plastic vessels were mixed in the ThermoMixer® comfort (~ 1000 rpm). These stirring rates ensured homogeneous mixing and mass transfer to Novozym 435 without mechanical damage to immobilized enzymes and without affecting the obtained reaction equilibria.

The reaction mixtures were prepared gravimetrically using a XS205 DualRange balance from Mettler Toledo (Colubus, USA) with an accuracy of $\pm 10^{-4}$ g. Every initial reaction mixture was prepared twice, so that each experimental reaction equilibrium position was obtained by biological duplicates. First, defined mass of alcohol (MeOH, EtOH, or 1-BuOH) was filled in the vessels and then defined weights of LA and water were added. Different amounts of water were added to the initial reaction mixtures because it was one aim of this work to study the effect of water on reaction equilibrium and on initial enzyme activity. Besides LA, the reacting alcohol, water and enzyme, and additional chemicals have not been added to the mixtures, meaning that no additional solvent was present and the reacting alcohol served simultaneously as solvent. The glass vessels were sealed with caps containing a septum for sampling or substrate addition; 5-mL syringes were used for these purposes. The plastic vessels were sealed and have been opened only when the minimum time for

Table 1 List of Symbols

Latin characters		
a	J mol ⁻¹	Helmholtz energy
a_i		Activity of component i
$c_{p,0i}^E$	J mol ⁻¹ ·K ⁻¹	Heat capacity of component i
g^E	kJ mol ⁻¹	Excess Gibbs energy
$\Delta^R g^0$	kJ mol ⁻¹	Standard Gibbs energy of reaction
$\Delta^F g_{0i}^0$	kJ mol ⁻¹	Standard Gibbs energy of formation of component i
$\Delta^R h^0$	kJ mol ⁻¹	Standard enthalpy of reaction
$\Delta^C h_{0i}^0$	kJ mol ⁻¹	Standard enthalpy of combustion of component i
$\Delta^F h_{0i}^0$	kJ mol ⁻¹	Standard enthalpy of formation of component i
Δh_{0i}^{LV}	kJ mol ⁻¹	Enthalpy of vaporization of component i
k_B	J·K ⁻¹	Boltzmann constant
k_{ij}		Binary interaction parameter for dispersion
k_{ij}^{WS}		Binary interaction parameter for association
K_{th}		Thermodynamic equilibrium constant
K_γ		Quotient of activity coefficients
K_x		Apparent equilibrium constant
M_i	g mol ⁻¹	Molecular weight
m_i^{seg}		Segment number of component i
N		Number of association sites
R	J mol ⁻¹ ·K ⁻¹	Ideal gas constant
$\Delta^F s_{0i}^0$	J mol ⁻¹ ·K ⁻¹	Entropy of formation of component i
Δs_{0i}^{LV}	J mol ⁻¹ ·K ⁻¹	Entropy of vaporization of component i
s_i^0	J mol ⁻¹ ·K ⁻¹	Standard entropy of component i
T	K	Temperature
u_i/k_B	K	Dispersion-energy parameter of component i
x_i		Mole fraction of component i
X		Conversion
Z		Compressibility factor
Greek characters		
ε^{AiBi}/k_B	K	Association-energy parameter of component i
κ^{AiBi}		Association-volume parameter of component i
ν_i		Stoichiometric coefficient
φ_i		Fugacity coefficient of component i
σ_i	Å	Segment diameter of component i
γ_i		Activity coefficient of component i
λ		Extent of reaction
Subscript		
$0i$		Pure component
i,j		Component indices
Superscript		
res		Residual
0		Standard state
R		Reaction
F		Formation
LV		Vaporization

equilibration of the reactions was reached. These times were determined as follows. Samples were taken after defined times of reactions (data not shown here) from the 10-mL glass vessels to study the time required for equilibration. This allowed

sampling from 1.5-mL plastic vessels at reaction times where reaction equilibrium condition was ensured. The amount of Novozym 435 was adjusted in all vessels gravimetrically by setting the enzyme activity to about 125 U/g solution. This was a compromise between a minimum amount of enzyme required for reasonable reaction rates on the one hand and mechanical damage on the other hand due to the presence of more immobilized enzyme that lead to highly heterogeneous reaction mixtures where mechanical damage of Novozym 435 was observed. The similarity of results for the two types of vessels has been ensured by comparing equilibrium results for two equal set-ups in the two vessel types (10 and 1.5 mL). It can be stated here that parameters of the reaction set up like type of vessel, stirring speed, and amount of enzyme have been studied in detail and were found to not influence the thermodynamic reaction equilibrium. Thus, the conditions under study apparently did not cause enzyme inactivation or mass transport limitations.

Mole fractions of the reacting agents at equilibrium were analyzed using two different analytical methods. The mole fraction of water was determined using Karl-Fisher titration with a Metrohm 915 KF Ti-Touch (Metrohm, Herisau, Switzerland). Each sample was measured in triplicate and the results were averaged. To quantify alkyl levulinates, a gas chromatography system was used that consisted of an Agilent Technology 7890A GC equipped with an Agilent INNOWax column (30 m, 0.32 mm, 0.5 mm) and a flame ionization detector. All measurements were performed in triplicate, while calibration was performed separately for each ester system.

Theory

Based on the equilibrium mole fractions, the standard Gibbs energy of reaction $\Delta^R g^0$ can be expressed via the thermodynamic equilibrium constant K_{th} of the reaction

$$\Delta^R g^0 = -R \cdot T \cdot \ln(K_{th}) \quad (1)$$

Here, R is the universal gas constant. Eq. (1) and (4) show how the thermodynamic equilibrium constant K_{th} is related to thermochemistry data of the reaction. K_{th} of an esterification of a monocarboxylic acid can be expressed via the thermodynamic activities of the products over the reactants

$$K_{th} = \prod_i a_i^{\nu_i} = \frac{a_{ester} \cdot a_{water}}{a_{levulinic\ acid} \cdot a_{alcohol}} \quad (2)$$

The activity a_i is defined as the product of the mole fraction and the respective mole-fraction-based activity coefficient of reacting agent i . Therefore Eq. (2) can be written as

$$K_{th} = K_x \cdot K_\gamma = \frac{x_{ester} \cdot x_{water}}{x_{levulinic\ acid} \cdot x_{alcohol}} \cdot \frac{\gamma_{ester} \cdot \gamma_{water}}{\gamma_{levulinic\ acid} \cdot \gamma_{alcohol}} \quad (3)$$

In Eqs. (2) and (3), esters studied in this work are methyl levulinate, ethyl levulinate, and butyl levulinate, and they belong to the alcohols MeOH, EtOH, and 1-BuOH, respectively. The mole fractions and thus K_x values are equilibrium properties, and thus have to be accessed through reaction equilibrium experiments. Activity coefficients are accessible by thermodynamic modeling.

The standard Gibbs energy of reaction $\Delta^R g^0$ can be expressed via the thermodynamic properties of reacting species:

$$\Delta^R g^0 = \sum_i \nu_i \cdot \Delta^F g_{0i}^0 \quad (4)$$

where ν_i denotes the stoichiometric coefficient and $\Delta^F g_{0i}^0$ the standard Gibbs energy of formation of a pure reacting agent i . The latter is usually obtained by

$$\Delta^F g_{0i}^0 = \Delta^F h_{0i}^0 - T \cdot \Delta^F s_{0i}^0 \quad (5)$$

where $\Delta^F h_{0i}^0$ is the standard enthalpy of formation and $\Delta^F s_{0i}^0$ the standard entropy of formation of the pure reacting agent i , and T is the absolute temperature in Kelvin. $\Delta^F s_{0i}^0$ can be calculated using the standard entropy of a pure reacting agent s_{0i}^0 and entropy of the elements $s_{element}^0$ (values see Table S9):

$$\Delta^F s_{0i}^0 = s_{0i}^0 + \sum_{elements} (\nu_{element} \cdot s_{element}^0) \quad (6)$$

where elements refer to the elements that form the respective reacting agent i . The temperature dependencies of thermodynamic properties were described in this work with

$$\Delta^F h_{0i}^0(T) = \Delta^F h_{0i}^0(T^0) + \int_{T^0}^T c_{p0i}^0(T) dT \quad (7)$$

$$s_{0i}^0(T) = s_{0i}^0(T^0) + \int_{T^0}^T \frac{c_{p0i}^0(T)}{T} dT \quad (8)$$

where $c_{p0i}^0(T)$ is the temperature-dependent heat capacity of the pure component i .

Thermochemical data on levulinic acid and alkyl levulinates required for calculation of the thermodynamic equilibrium constants of the LA esterification with alcohols are compiled in Tables S7–S10 (Fig. 1).

PC-SAFT

PC-SAFT is based on the perturbation theory of Barker and Henderson (Barker and Henderson 1967) and calculates the residual Helmholtz energy a^{res} of a system. The molecules are regarded as chains of hard spheres (hard chain), which represents the reference system and accounts for repulsive interactions. Perturbations due to attractive Helmholtz energy contributions in form of dispersive van der Waals attraction (dispersion) and



Fig. 1 Scheme of the esterification of levulinic acid (LA) with alcohols ($R = \text{CH}_3$ or CH_2CH_3 or $(\text{CH}_2)_3\text{CH}_3$). Provenance and purity of compounds used in this study are listed in Table S1

hydrogen bonds (association) are added to $a^{\text{hard chain}}$ yielding

$$a^{\text{res}} = a^{\text{hard chain}} + a^{\text{dispersion}} + a^{\text{association}} \quad (9)$$

Within PC-SAFT, a component i is characterized by a set of pure-component parameters. It is described as a chain of m_i^{seg} segments with a specific segment diameter σ_i . The chains interact via dispersion forces, which are accounted for by the dispersion-energy parameter $\frac{u_i}{k_B}$, where k_B is the Boltzmann constant. Association interactions are described by the two parameters association-energy parameter $\frac{\epsilon^{\text{AiBi}}}{k_B}$ and association-volume parameter κ^{AiBi} , and a molecule is ascribed a certain number of associating sites N . This means that for an associating component, five parameters are required and for a non-associating component three parameters, respectively. These pure-component parameters are obtained by regression to vapor-pressure data and liquid-density data of pure components.

For the description of mixtures, mixing rules have to be applied. Lorentz-Berthelot combining rules were applied for the segment diameter σ_{ij} and the dispersion-energy parameter u_{ij}

$$\sigma_{ij} = \frac{1}{2}(\sigma_i + \sigma_j) \quad (10)$$

$$u_{ij} = \sqrt{u_i u_j} \cdot (1 - k_{ij}) \quad (11)$$

Further, Wolbach-Sandler (Wolbach and Sandler 1998) mixing rules were applied to the association parameters:

$$\epsilon^{\text{AiBj}} = \frac{1}{2}(\epsilon^{\text{AiBi}} + \epsilon^{\text{AjBj}}) \cdot (1 - k_{ij}^{\text{ws}}) \quad (12)$$

$$\kappa^{\text{AiBj}} = \sqrt{\kappa^{\text{AiBi}} \kappa^{\text{AjBj}}} \cdot \left(\frac{\sqrt{\sigma_i \sigma_j}}{\frac{1}{2}(\sigma_i + \sigma_j)} \right)^3 \quad (13)$$

As it can be observed, two binary parameters are present in these combining rules k_{ij} and k_{ij}^{ws} which are binary interaction parameters between two components i and j . These parameters can be adjusted to binary phase equilibria like vapor-liquid, liquid-liquid, or solid-liquid equilibria. In general, binary interaction parameters can be expressed as temperature-dependent functions:

$$k_{ij} = k_{ij,m} \cdot T + k_{ij,b} \quad (14)$$

Once PC-SAFT pure-component parameters and binary parameters are available, activity coefficients can be obtained via fugacity coefficients φ_i of a component i in mixture divided by the fugacity coefficient φ_{0i} of the pure component $0i$:

$$\gamma_i = \frac{\varphi_i(T, p, \bar{x})}{\varphi_{0i}(T, p, x_i = 1)} \quad (15)$$

The fugacity coefficient can be obtained as function of residual Helmholtz energy and derivations of a^{res} with respect to mole fraction and number density.

Results

Pure-component PC-SAFT parameters

PC-SAFT parameters have to be known prior to predict K_y values that are required in Eq. (3). First, pure-component parameters of all components present in the reaction have to be estimated, except for Novozym 435 which is neglected in modeling due to the very low concentration in the reaction mixtures. PC-SAFT pure-component parameters for LA and the three corresponding alkyl levulinates were not available in the literature and were fitted in this work. The pure-component parameters for the alcohols MeOH, EtOH, and 1-BuOH and for water are available in literature and are summarized in Table S5. The pure-component parameters were adjusted in this work to experimental density and vapor pressure data of pure components using the following objective function:

$$OF1 = \sum_{k=1}^{\text{NP}_{\rho_{0i}^{LV}}} \left| \left(1 - \left(\frac{\rho_{0i}^{LV, \text{calc}}}{\rho_{0i}^{LV, \text{exp}}} \right)_k \right)^2 \right| + \sum_{m=1}^{\text{NP}_{\rho_{0i}}} \left| \left(1 - \left(\frac{\rho_{0i}^{\text{calc}}}{\rho_{0i}^{\text{exp}}} \right)_m \right)^2 \right| \quad (16)$$

The acid LA was treated as self-associating component; the levulinates were regarded as induced associating components. In the concept of induced association, it is assumed that the regarded molecule must not interact via self-association, but only via cross-association with other self-associating components. This means, five pure-component parameters were fitted for LA, and three for each alkyl levulinate. The so-determined PC-SAFT parameters are summarized in Table S5.

The comparison between experimental density data and PC-SAFT modeling results is illustrated in Fig. 2a, and a very good agreement can be observed. This statement is also valid for the pure-component vapor pressures, as shown in Fig. 2b.

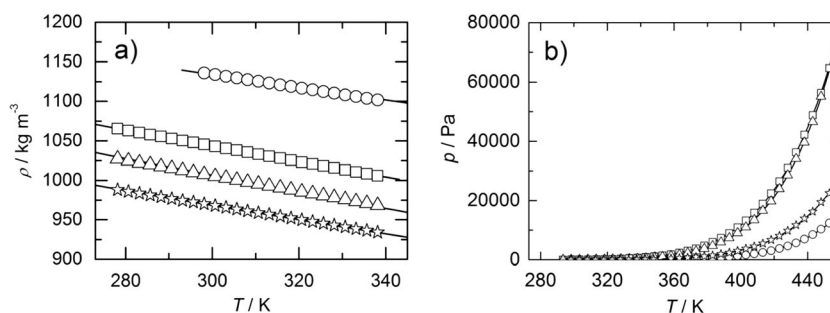


Fig. 2 Liquid densities **a** and vapor pressure **b** of LA and alkyl levulinates. Symbols are experimental data (circles LA, squares MLA, triangles ELA, stars BLA), and lines show PC-SAFT calculations using

parameters from Table S5. Experimental data of LA, ELA, and BLA retrieved from (Lomba et al. 2011) and of MLA from (Lomba et al. 2013)

Binary PC-SAFT parameters

Besides pure-component parameters, binary parameters were adjusted prior to modeling multi-component reaction mixtures. For that purpose, phase equilibria of binary mixtures were used to determine binary interaction parameters k_{ij} (and additional k_{ij}^{ws} for some binary mixtures) required in Eqs. (11) and (12). For one neat esterification mixture consisting of four reacting agents (LA, alcohol, water, alkyl levulinate), six binary pairs exist. This yields 16 binary pairs since three esterification mixtures were considered in this work. Experimental data for liquid-liquid equilibria (LLE) and vapor-liquid equilibria (VLE) of binary mixtures were used to adjust the binary interaction parameters. Table S6 summarizes all binary mixtures investigated in this work. Phase-equilibrium data of these binary systems were partly available in literature. However, data for some binary mixtures were not available in the literature. The strategy then was either to predict the phase equilibria of those mixtures with UNIFAC (like the approach Chung et al. (Chung et al. 2015) use, especially binary mixtures containing either MeOH or methyl levulinate), or to measure them in this work, or to use LLE data of ternary systems stemming from literature as shown in Fig. S1. The binary parameters that were adjusted in this work to the respective phase-equilibrium data, and the deviation

between PC-SAFT modeling results and data sources in terms of ARD, are further listed in Table S6. To illustrate the accuracy of PC-SAFT modeling results, Fig. 3 compares the experimental VLE data of the system 1-BuOH/BLA and the experimental LLE data of the system H₂O/BLA (measured in this work) with the PC-SAFT modeling. The binary mixtures H₂O/EtOH and H₂O/1-BuOH have been modeled in previous works and the corresponding binary interaction parameters k_{ij} were inherited from literature (Altuntepe et al. 2017b).

LA esterification reaction: thermodynamic standard data at 323.15 K

In order to obtain reliable and consistent standard data, standard molar enthalpy and standard molar Gibbs energy of the LA esterification reaction have been derived from three different methods: from the reaction equilibrium data measured in this work (see Tables S2–S4), from thermochemical properties of the LA esterification reaction participants, as well as by assessment of the thermodynamic values by using a group contribution method (GCM) developed by Domalski and Hearing (Domalski and Hearing 1993). Admittedly, comparison of thermodynamic results has to be performed at any common temperature. While the reaction equilibrium

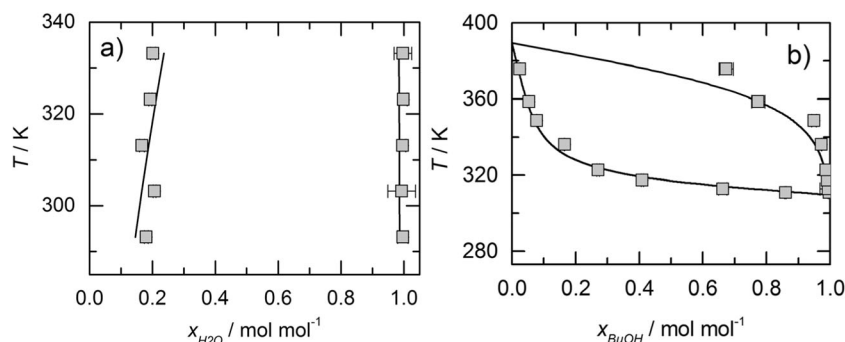


Fig. 3 **a** Experimental liquid-liquid equilibrium of the mixture water/BLA at atmospheric pressure. **b** Experimental vapor-liquid equilibrium of the mixture 1-BuOH/BLA at 0.02 bar determined in this work, with

uncertainty $u(x) = 0.0252$ and $u(T) = (0.15 + 0.002(T - 273.15))$ K. Lines are PC-SAFT calculations performed with the parameters summarized in Tables S5 and S6

measurements were carried out in this work at 323.15 K, it was necessary to use this temperature for the thermodynamic analysis and all required thermodynamic properties (see Table 2) were adjusted to 323.15 K. The adjustment was performed using heat capacities estimated by the well-established procedure by Ruzicka and Domalski (Rüžička and Domalski 1993). Thermodynamic properties of water and alcohols (MeOH, EtOH, and 1-BuOH) used in this work were taken from the literature (see Tables S7 and S8). Thermodynamic properties of LA were taken from our previous work (Verevkin and Emel'yanenko 2012). Thermodynamic data for the methyl levulinate (MLA), ethyl levulinate (ELA), and butyl levulinate (BLA) have been measured in our recent work (Emel'yanenko et al., personal communication). Compilation of the thermodynamic properties at 323.15 K used in this work is given in Table 2.

The group contribution methods are commonly useful tools for a first estimate of formation properties, but these values are often inaccurate. As it can be seen in Table 2, the thermodynamic properties of LA esters estimated by GCM are significantly different from the experimental data. As a consequence, the equilibrium constants derived from the GCM data are at least twice overestimated in comparison to the reliable data measured in this work. For example, the standard Gibbs energy of the LA esterification reaction with MeOH is $\Delta^R g^0 = -13.85 \text{ kJ mol}^{-1}$ and was calculated from the GCM results given in Table 2. The thermodynamic equilibrium constant $K_{th} = 173.2$ was derived from the GCM estimates. The standard Gibbs energy of the same reaction $\Delta^R g^0 = -11.79 \text{ kJ mol}^{-1}$ (see Table 2) and the corresponding value $K_{th} = 80.5$ clearly demonstrates the failing of the GCM to predict equilibrium constants accurately.

Considering Table 2, it can be stated that $\Delta^R g^0$ from GCM and from the experimental thermochemistry data are only in

qualitative agreement. Both methods consistently predict $\Delta^R g^0$ values in the order $\Delta^R g^0$ (MeOH) < $\Delta^R g^0$ (EtOH) < $\Delta^R g^0$ (BuOH). Gibbs energies of reaction $\Delta^R g^0$ estimated with GCM are very similar for the reactions under consideration, but they are significantly more negative than $\Delta^R g^0$ values derived from our thermodynamic study based on measurements from (Emel'yanenko et al., personal communication).

Equilibrium concentrations for the reactions under investigation were measured in a first step at different reaction conditions in order to have a broad data basis. The initial mole fractions of water and LA were varied in the different batches. After reaction equilibrium was reached, samples were taken and analyzed. The measured equilibrium mole fractions were used to calculate K_x (Eq. (3)). The range of K_x values was rather small due to the high excess of alcohol in the reaction mixtures. The results on K_x values are listed in Tables S2–S4. In order to obtain K_γ (Eq. (3)), the activity coefficients were predicted by PC-SAFT (see Tables S2–S4). It has turned out that K_x values ranged from 0.1 to 2 and the corresponding K_γ values ranged from 45 to 103 for the different reaction conditions of LA esterification with MeOH. With EtOH (1-BuOH), K_x ranges between 0.4 and 0.8 (0.1 and 2) and K_γ between 12 and 15 (2 and 8) for the different reaction conditions. For each different reaction, all K_x values were multiplied with predicted K_γ values, resulting in an averaged K_{th} value for the individual reactions. At 323.15 K, the so-obtained K_{th} values were found to be 36 ± 28 for LA esterification with MeOH, 8.9 ± 5.4 for LA esterification with EtOH, and 5.1 ± 2.8 for LA esterification with 1-BuOH, respectively. The given range of confidence is caused by experimental uncertainty of K_x as well as the fact that many K_x values were used to derive K_{th} values (see Fig. 4).

Table 2 Thermochemistry data used in this work, originating from experimental determinations (data compiled with sources in Tables S7–S10) and from the group contribution method (GCM) of Domalski and Hearing (Domalski and Hearing 1993) at 323.15 K. The heat capacities that are required for determinations at 323.15 K were estimated with the method of Ruzicka and Domalski (Rüžička and Domalski 1993). $\Delta^R g^0$ indicates the Gibbs energy of reaction of each esterification reaction calculated with the corresponding values of alcohol, water, LA, and ester

Compound	$\Delta^F h_{0i}^0$ [kJ mol ⁻¹]	s_{0i}^0 [J mol ⁻¹ ·K ⁻¹]	$\Delta^F g_{0i}^0$ [kJ mol ⁻¹]	$\Delta^R g^0$ [kJ mol ⁻¹]
Experimental				
H ₂ O	-283.95	76.02	-232.08	
MeOH	-236.30	133.94	-158.14	
EtOH	-273.89	169.79	-162.29	
1-BuOH	-323.49	240.56	-144.73	
LA	-677.94	286.27	-487.78	
MLA	-645.07	334.98	-425.63	-11.79
ELA	-678.96	364.35	-423.99	-6.00
BLA	-728.14	425.65	-402.95	-2.52
Group contribution method				
LA	-677.80	286.72	-487.78	
MLA	-635.42	371.23	-427.69	-13.85
ELA	-670.51	406.09	-429.03	-11.03
BLA	-720.45	475.75	-411.45	-11.01

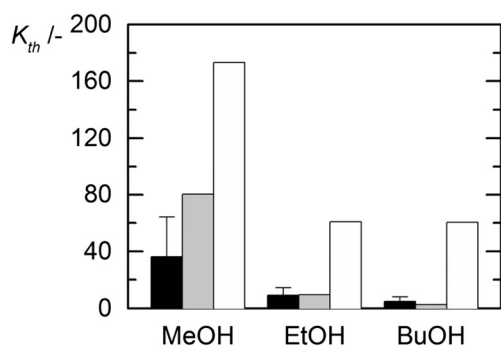


Fig. 4 Thermodynamic equilibrium constants of LA esterifications at 323.15 K for the MeOH-, EtOH-, and 1-BuOH esterification. Black: determination via reaction equilibrium experiments with PC-SAFT calculations, gray: determination via experimental thermochemical data from (Emel'yanenko et al., personal communication), and white: estimation via group contribution method of Domalski and Hearing (Domalski and Hearing 1993)

Water influence on reaction equilibrium

One of the aims of this work was to apply thermodynamics to understand the role of water for LA esterification. Water is a key component in enzyme-catalyzed esterifications because it affects both enzyme kinetics and reaction equilibrium. In previous works, it was shown that a slice amount of water in organic reaction medium has a positive effect on Lipase activity (see for example (Altuntepe et al. 2017a)). Nevertheless, more water in the feed composition will shift the reaction equilibrium of any esterification to the reactant side. Thus, the initial water content was varied in different reaction batches in order to quantify the effect of water on reaction equilibrium.

Three different reaction mixtures were prepared that contained the same initial LA concentration but three different initial water mole fractions. The equilibrium compositions were measured, and K_x and LA conversion were calculated from that data. The results for LA esterification with EtOH are summarized in Fig. 5.

From the experimental data in Fig. 5a, it gets obvious that the conversion of LA decreases with increasing initial water

mole fraction. This is due to the shift of the reaction equilibrium to the reactant side with increasing amount of water in the reaction mixture.

Influence of LA concentration on reaction equilibrium

Next, the effect of LA concentration in the initial reaction mixtures on reaction equilibrium was investigated. For this, experiments were performed for LA esterifications with MeOH, EtOH, and 1-BuOH (data shown in Tables S2–S4) at rather low LA concentrations. It can be observed from the data that only slightly varying LA content in the reaction feeds does not have an influence on K_x and on LA conversion. Thus, experiments were performed also for significantly higher LA contents in the reaction mixtures of LA esterification with 1-BuOH. The initial mole-fraction ratio of 1-BuOH to LA was set to 1:3, 1:1, or to 3:1. The results are summarized in Table 3. Please note that a small amount of water was added to each initial reaction mixture.

The experimental results show an unexpected behavior. While excess of 1-BuOH over LA (3:1) strongly shifts the reaction equilibrium to the product side (higher K_x) compared to equimolar reaction mixtures (1:1), the opposite was found for excess of LA over 1-BuOH (3:1). This can be observed in Fig. 6a for the K_x values and in Fig. 6b for conversion of LA and 1-BuOH in dependence of ratio of 1-BuOH over LA in the initial reaction mixtures. It can be observed that conversion of LA increases with increasing 1-BuOH content, whereas 1-BuOH conversion slightly decreases (see Fig. 6b). This behavior can only be explained by molecular interactions, expressed in activity coefficients.

Predicting LA conversion

The main focus of this work has been to predict LA conversions, X_{LA} , at equilibrium (maximum conversion) depending on the different initial reaction conditions and to

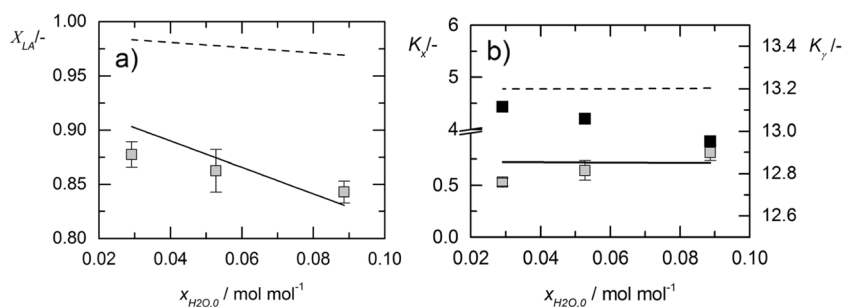


Fig. 5 **a** Experimental and predicted equilibrium conversion of LA in dependence of the initial water mole fraction in the reaction mixture. Solid line: PC-SAFT prediction with K_{th} from experimental thermochemistry data and dashed line: PC-SAFT prediction with K_{th} from GCM. **b** Experimental apparent equilibrium constant K_x (gray

squares—left axis) and K_γ (black squares—right axis) in dependence of the initial water mole fraction in the reaction mixture. Lines: PC-SAFT prediction of K_x using K_{th} from experimental thermochemistry data (solid line) or from GCM (dashed line)

Table 3 Summary of the results for the three different batches of the initial 1-BuOH/LA ratio variation. The initial mole fractions of 1-BuOH and LA are given, which do not sum to one caused by the presence of small amounts of water. Further the equilibrium compositions, K_x , the LA conversion, activity coefficients of reactants at equilibrium, and K_γ are summarized. The predicted equilibrium compositions and predicted K_x and LA conversions X_{LA} are shown as well, with X_{LA} being the main result (presented in italic)

	$\frac{x_{BuOH,0}}{x_{LA,0}}$	1:3	1:1	3:1	
Initial mole fractions	$x_{LA,0}$	0.7073	0.4788	0.2421	
	$x_{BuOH,0}$	0.2351	0.4733	0.7130	
Reaction equilibrium experiments	x_{LA}	0.6357	0.3874	0.0501	
	x_{BuOH}	0.1635	0.3818	0.5211	
	x_{H2O}	0.1292	0.1394	0.2368	
	x_{BLA}	0.0717	0.0914	0.1920	
	K_x	0.0891	0.0861	1.7409	
	X_{LA}	<i>0.1013</i>	<i>0.1909</i>	<i>0.7930</i>	
	γ_{LA}	1.0407	1.1485	1.4020	
	γ_{BuOH}	1.2859	1.1089	0.9870	
	γ_{H2O}	2.6975	3.1303	3.7602	
	γ_{BLA}	3.9151	2.7123	2.2634	
Prediction using $K_\gamma^{PC-SAFT}$ and K_{th} from thermochemistry	K_γ	7.8911	6.6665	6.1505	
	x_{LA}	0.5881	0.3194	0.1004	
	x_{BuOH}	0.1152	0.3047	0.5777	
	x_{H2O}	0.1772	0.2120	0.1826	
	x_{BLA}	0.1195	0.1639	0.1394	
	K_x	0.3126	0.3571	0.4390	
	X_{LA}	<i>0.1689</i>	<i>0.3391</i>	<i>0.5814</i>	
	Prediction using $K_\gamma^{PC-SAFT}$ and K_{th} from GCM	x_{LA}	0.4908	0.1448	0.0132
		x_{BuOH}	0.0180	0.1302	0.4905
		x_{H2O}	0.2745	0.3866	0.2698
x_{BLA}		0.2167	0.3385	0.2266	
K_x		6.7368	6.9410	9.4713	
X_{LA}		<i>0.3063</i>	<i>0.7003</i>	<i>0.9451</i>	

compare these predictions with experimental data. Esterification of LA with 1-BuOH is chosen to demonstrate the procedure in the following. A strategy was developed to predict equilibrium compositions of reaction mixtures yielding K_x^{pred} values by minimizing the following objective function at constant temperature

$$OF(\lambda) = \left| K_{th} - \left(K_x^{pred}(\lambda) \cdot K_\gamma^{PC-SAFT}(\lambda) \right) \right| = \min \quad (17)$$

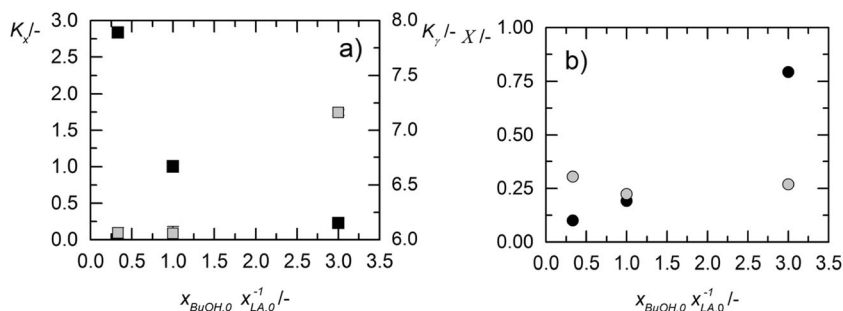


Fig. 6 **a** Experimental apparent equilibrium constant K_x (gray squares) and ratio of reacting agents' activity coefficients K_γ (black squares—right axis) in dependence of the initial 1-BuOH/LA ratio. **b** LA conversion

In Eq. (17), the thermodynamic equilibrium constant K_{th} has to be known. This value was inherited from the data presented in Fig. 4 using either thermochemical experimental data or GCM results. The activity coefficients of the reacting agents were predicted with PC-SAFT using the parameters in Tables S5 and S6 to quantify $K_\gamma^{PC-SAFT}$. Equation (17) is a function of the extent of reaction λ that relates the input initial composition of the reacting agents (index 0) with the equilibrium mole fractions of the reacting agents based on the stoichiometry of the reaction:

$$x_{LA} = x_{LA,0} - \lambda \quad (18)$$

$$x_{1-BuOH} = x_{1-BuOH,0} - \lambda \quad (19)$$

$$x_{BLA} = \lambda \quad (20)$$

$$x_{water} = x_{water,0} + \lambda \quad (21)$$

Eqs. (17)–(21) yield λ at equilibrium and thus predicted equilibrium compositions that need experimental validation. These experimental data were taken from Fig. 5 and in Table 3. The equilibrium data were measured for different mole fractions of LA and water in the initial reaction mixtures.

Influence of temperature on K_{th}

All reaction equilibrium measurements in this work have been performed only at 323.15 K. However, all required thermodynamic standard data for predicting conversions are temperature dependent. Modeling temperature dependence of K_{th} values requires enthalpy data and heat capacities. For alkyl levulinates, LA, and alcohols, the latter were calculated with the method of Ruzicka and Domalski (Růžička and Domalski 1993). For water, all required temperature-dependent thermodynamic properties were taken from Chase (Chase 1998). All these data were used to determine $\Delta^R g^0$ with Eq. (4) at 298.15 K. Standard thermodynamic relations (Eqs. (5)–(8)) were then applied to calculate the temperature dependence of $\Delta^R g^0$, and thus the respective K_{th} . So-obtained K_{th} values are illustrated in Fig. 7 and compared with K_{th} at 323.15 K (inherited from

(black circles) and 1-BuOH conversion (gray squares) in dependence of the initial 1-BuOH/LA ratio

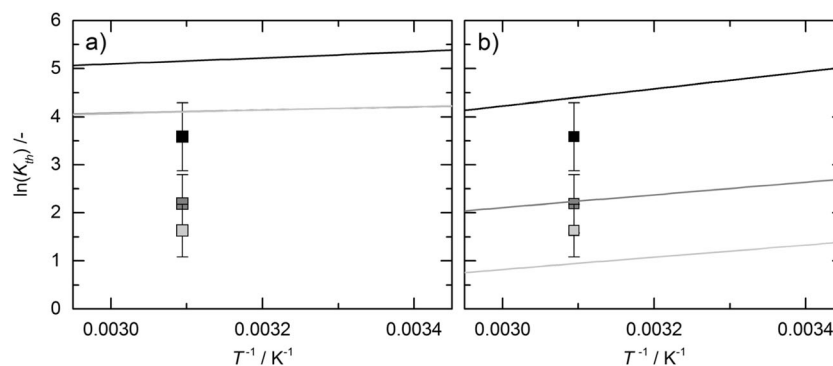


Fig. 7 Summary of the K_{th} values in dependence of the reaction temperature. Squares are results from reaction equilibrium determinations with PC-SAFT calculations of activity coefficients. Black: MeOH esterification, dark gray:

EtOH esterification, and bright gray: 1-BuOH esterification. Lines: **a** K_{th} via GCM (**b**) K_{th} via experimental formation properties

the data presented in Fig. 4) with the respective confidence range.

Figure 7 illustrates once again that K_{th} values from GCM significantly overestimate K_{th} values from thermochemical data on alkyl levulinates (Emel'yanenko et al., personal communication) as well as from experimental reaction equilibrium data measured in this work that were combined with PC-SAFT predicted $K_{\gamma}^{PC-SAFT}$ values. Nevertheless, the obtained results are remarkable considering the fact that many different independent methods and data (experimental thermochemical properties, heat capacity estimations, reaction equilibrium measurements, and activity coefficient predictions) were used to consistently predict reaction equilibria of enzyme-catalyzed LA esterification.

Discussion

Standard data of LA esterification

The obvious deviation that is described in Table 2 is discussed by comparing the shown $\Delta^R g^0$ data with $\Delta^R g^0$ values from reaction equilibrium experiments and activity coefficients. This is possible because the activity-based equilibrium constant is related to $\Delta^R g^0$ by Eq. (1). As activity is defined by concentration times activity coefficients, experiments and thermodynamic modeling were performed.

The fact that the activity coefficients are strongly non-unity shows that K_x strongly depends on concentration, and the reaction mixtures for LA esterification in MeOH are strongly non-ideal, caused by molecular interactions. This supports findings from other works that observed that esterification mixtures strongly deviate from ideality (see (Altuntepe et al. 2017a; Grob and Hasse 2005; Riechert et al. 2015)). Considering K_{γ} values, it can be stated that the non-ideality of the reaction mixtures decreases (K_{γ} values get closer to one) from MeOH to 1-BuOH. This is a reasonable observation as

LA is a C5 acid, and mixtures of LA with small molecules (such as MeOH) usually demonstrate significant deviation from ideal-mixture behavior.

The K_{th} values of the LA esterification reactions with alcohols obtained from K_{γ} and K_x were further compared with equilibrium constants estimated by GCM and with those obtained by experimental formation data in Fig. 4. It can be observed from Fig. 4 that K_{th} calculated from reaction equilibrium data measured in this work and activity coefficients predicted by PC-SAFT is in very good agreement with the K_{th} values derived from experimental thermochemical data on LA and its esters measured in our recent work by combustion calorimetry and transpiration method (Emel'yanenko et al., personal communication). In contrast, the K_{th} values estimated with the GCM significantly deviate from the both experimental determinations. Thus, it can be stated that K_{th} from reaction equilibrium data and activity coefficient predictions are cross-validated with experimental formation properties, and that the use of GCMs should be avoided if other data are available.

Water influence on LA conversion

In Fig. 5b, an unexpected dependence of K_x values on water content is observed. It is expected that K_x decreases with the shift of the equilibrium to the reactant side, which is obviously contrary to the experimental results. The reason for the fact that K_x increases with increasing mole fraction of water in the feed is the excess of EtOH in the reaction mixture compared to a relatively low water content, which obviously compensates the effect of water. Further, higher x_{H_2O} values cause decreased LA conversion and increased K_x because of the definition in Eq. (3). This effect is dominating at low water mole fractions, while K_x might indeed decrease with increasing x_{H_2O} for higher initial water content. To summarize, it can be stated that a decrease in LA conversion does not necessarily cause a decreased K_x and vice versa. Similar behaviors were observed also for LA esterification with MeOH and with 1-BuOH (see Tables S2–S4).

The formalism presented in Eqs. (17)–(21) were further used to predict LA conversion. Comparing experimental LA conversions with the predictions using K_{th} from experimental thermochemical formation, data are in very good agreement with experimental results. In contrast, the predicted LA conversions with K_{th} estimated from GCM significantly overestimated the experimental LA conversions. Nevertheless, the qualitative dependence of the water content on LA conversion is described correctly with Eqs. (17)–(21) using K_{th} from GCM. The deviations are caused by too high K_{th} value, which therefore results in LA mole fractions that were then significantly too low. These results point out to the importance of accurate and consistent K_{th} values, and they explain the errors obtained by using inconsistent K_{th} values.

Influence of ratio 1-BuOH:LA on LA conversion

Next to the water influence on reaction equilibrium, the influence of the ratio 1-BuOH:LA in the initial reaction mixtures was predicted. Since K_{th} is only a function of temperature, the product of K_x and K_γ has to be constant in order to fulfill Eq. (17). As it could be observed from Fig. 6, K_x values increased upon increasing initial 1-BuOH:LA ratio. Thus, K_γ is expected to decrease upon increasing initial 1-BuOH:LA ratio. As it can be seen in Fig. 6, this was exactly obtained with activity coefficients of the reacting agents predicted with PC-SAFT. That is, the concentration dependence of LA conversion that has been observed experimentally can be explained with activity coefficients of the reacting agents, or in other words, with the molecular interactions which are strongly non-ideal in esterification mixtures. The summarized prediction results are listed in Table 3 and compared to experimental LA conversion data in dependence of the initial mole-fraction ratio 1-BuOH/LA.

It can be observed from Table 3 that the experimental LA conversion increases with increasing excess of 1-BuOH in the initial reaction mixtures from 0.10 (ratio 1:3) to 0.19 (ratio 1:1) to 0.79 (ratio 3:1). These experimental results predicted with the formalism in Eqs. (17)–(21) were qualitatively correct using activity coefficients from PC-SAFT and K_{th} value obtained either from GCM or from thermochemistry. However, distinct quantitative differences between results obtained with K_{th} from GCM or from thermochemistry in Eq. (17) can be observed. K_{th} from GCM ($K_{th} = 60.3$) significantly overestimated LA conversion. This is due to the comparably high K_{th} value. In contrast, using activity coefficients from PC-SAFT and K_{th} of 2.6 from thermochemistry allow predicting LA conversions that are in very good agreement to the experimental data.

As summary, it can be stated that reaction equilibria and maximum LA conversion as function of different reaction conditions could be predicted with the formalism presented in this work. This formalism requires the thermodynamic

equilibrium constant K_{th} , accessible from a group contribution method for Gibbs energy of formation, experimentally determined formation properties, and reaction equilibrium measurements accompanied by activity coefficient predictions using PC-SAFT. The K_{th} values obtained from the experimental methods were found to be in good agreement but significant disagreement was observed for the K_{th} values estimated from Gibbs energy of formation obtained with group contribution method. Further, the experimental K_{th} values were used in order to determine the reaction coordinate and thus, finally to determine LA conversion. Activity coefficients required for the thermodynamic interpretation of the equilibrium studies have been predicted by PC-SAFT. Required model parameters were either available from literature or determined in this work from reaction-independent phase-equilibrium data. Modeling revealed that for the investigated reaction mixtures activity coefficients significantly deviated from unity caused by strong molecular interactions. This caused increasing LA conversion data upon increasing 1-BuOH excess and upon decreasing the water content in the initial reaction mixtures. Accounting for these strong non-ideal behaviors by predicting the activity coefficients with PC-SAFT allowed predicting LA conversion in very good agreement with the experimental observations. For this, experimental K_{th} values from experimental formation properties were used. In contrast, distinct deviations to the experimental LA conversions were observed if K_{th} values were used that have been estimated by group contribution method.

To conclude, bringing thermodynamic modeling with PC-SAFT together with experimental thermochemistry data enabled precise prediction of equilibrium compositions and thus K_x and LA equilibrium conversions. The initial feed compositions, thermodynamic equilibrium constant, and activity coefficients are required for that. Note, that the modeling with PC-SAFT was parametrized to reaction-independent phase-equilibrium data.

Acknowledgements This work was supported by the German Science Foundation (Leibniz award to G. Sadowski). The authors moreover acknowledge support by the Cluster of Excellence RESOLV (EXC 1069) funded by the Deutsche Forschungsgemeinschaft (DFG). This work was also partly supported by the Government of Russian Federation (decree №220 of 9 April 2009), agreement №14.Z50.31.0038.

Compliance with ethical standards This article does not contain any studies with human participants or animals performed by any of the authors.

Conflict of interest The authors declare that they have no conflict of interest.

References

- Alonso DM, Bond JQ, Dumesic JA (2010) Catalytic conversion of biomass to biofuels. *Green Chem* 12(9):1493–1513
- Altuntepe E, Greinert T, Hartmann F, Sadowski G, Held C (2017a) Thermodynamics of enzyme-catalyzed esterifications: I. Succinic acid esterification with ethanol. *Appl Microbiol Biotechnol* 101: 5973–5984
- Altuntepe E, Reinhardt A, Brinkmann J, Briesemann T, Sadowski G, Held C (2017b) Phase behavior of binary mixtures containing succinic acid or its esters. *J Chem Eng Data* 62:1983–1993
- Barker JA, Henderson D (1967) Perturbation theory and equation of state for fluids: the square-well potential. *J Chem Phys* 47(8):2856–2861
- Bart H, Reidtschläger J, Schatka K, Lehmann A (1994) Kinetics of esterification of succinic anhydride with methanol by homogeneous catalysis. In *J Chem Kinet* 26(10):1013–1021
- Bozell JJ, Moens L, Elliott D, Wang Y, Neuenschwander G, Fitzpatrick S, Bilski R, Jamefeld J (2000) Production of levulinic acid and use as a platform chemical for derived products. *Resour Conserv Recy* 28(3):227–239
- Chase MW (1998) NIST-JANAF thermochemical tables, 4 edn. American Chemical Society; American Institute of Physics for the National Institute of Standards and Technology, [Washington, D.C.], Woodbury, N.Y
- Christensen E, Williams A, Paul S, Burton S, McCormick RL (2011) Properties and performance of levulinate esters as diesel blend components. *Energy Fuel* 25(11):5422–5428
- Chung Y-H, Peng T-H, Lee H-Y, Chen C-L, Chien I-L (2015) Design and control of reactive distillation system for esterification of levulinic acid and n-butanol. *Ind Eng Chem Res* 54(13):3341–3354
- Climent MJ, Corma A, Iborra S (2014) Conversion of biomass platform molecules into fuel additives and liquid hydrocarbon fuels. *Green Chem* 16(2):516–547
- Dautzenberg G, Gerhardt M, Kamm B (2011) Bio based fuels and fuel additives from lignocellulose feedstock via the production of levulinic acid and furfural. *Holzforchung* 65(4):439–451
- Demma Carà P, Ciriminna R, Shiju N, Rothenberg G, Pagliaro M (2014) Enhanced heterogeneous catalytic conversion of furfuryl alcohol into butyl levulinate. *ChemSusChem* 7(3):835–840
- Démolis A, Essayem N, Rataboul F (2014) Synthesis and applications of alkyl levulinates. *ACS Sustain Chem Eng* 2(6):1338–1352
- Domalski ES, Hearing ED (1993) Estimation of the thermodynamic properties of C-H-N-O-S-halogen compounds at 298.15 K. *J Phys Chem Ref Data* 22(4):805–1159
- Grob S, Hasse H (2005) Thermodynamics of phase and chemical equilibrium in a strongly nonideal esterification system. *J Chem Eng Data* 50(1):92–101
- Gross J, Sadowski G (2001) Perturbed-chain SAFT: an equation of state based on a perturbation theory for chain molecules. *Ind Eng Chem Res* 40(4):1244–1260
- Gross J, Sadowski G (2002) Application of the perturbed-chain SAFT equation of state to associating systems. *Ind Eng Chem Res* 41(22): 5510–5515
- Hayes DJ (2009) An examination of biorefining processes, catalysts and challenges. *Catal Today* 145(1):138–151
- Hoffmann P, Voges M, Held C, Sadowski G (2013) The role of activity coefficients in bioreaction equilibria: thermodynamics of methyl ferulate hydrolysis. *Biophys Chem* 173:21–30
- Isikgor FH, Becer CR (2015) Lignocellulosic biomass: a sustainable platform for the production of bio-based chemicals and polymers. *Polym Chem* 6(25):4497–4559
- Kamm B, Gruber PR, Kamm M (2000) Biorefineries—industrial processes and products Ullman's encyclopedia of industrial chemistry. Wiley-VCH Verlag GmbH & Co. KGaA
- Kobayashi H, Fukuoka A (2013) Synthesis and utilisation of sugar compounds derived from lignocellulosic biomass. *Green Chem* 15(7): 1740–1763
- Lee A, Chaibakhsh N, Rahman MBA, Basri M, Tejo BA (2010) Optimized enzymatic synthesis of levulinate ester in solvent-free system. *Ind Crop Prod* 32(3):246–251
- Leibig C, Mullen B, Mullen T, Rieth L, Badarinarayana V (2011) Cellulosic-derived levulinic ketal esters: a new building block renewable and sustainable polymers. ACS Symposium Series, vol 1063. American Chemical Society, pp 111–116
- Lilly MD (1994) Eighth PV Danckwerts memorial lecture presented at Glaziers' Hall, London, UK 13 May 1993: Advances in biotransformation processes. *Chem Eng Sci* 49(2):151–159
- Lomba L, Giner B, Bandrés I, Lafuente C, Pino MR (2011) Physicochemical properties of green solvents derived from biomass. *Green Chem* 13(8):2062–2070
- Lomba L, Lafuente C, García-Mardones M, Gascón I, Giner B (2013) Thermophysical study of methyl levulinate. *J Chem Thermodyn* 65: 34–41
- Olson ES (2001) Conversion of lignocellulosic material to chemicals and fuels. National Energy Technology Lab., Pittsburgh, PA (US); National Energy Technology Lab., Morgantown, WV (US)
- Olson ES, Kjelden MR, Schlag AJ, Sharma RK (2001) Levulinate esters from biomass wastes chemicals and materials from renewable resources. ACS symposium series, vol 784. American Chemical Society, pp 51–63
- Petersson AEV, Gustafsson LM, Nordblad M, Borjesson P, Mattiasson B, Adlercreutz P (2005) Wax esters produced by solvent-free energy-efficient enzymatic synthesis and their applicability as wood coatings. *Green Chem* 7(12):837–843
- Pileidis FD, Titirici MM (2016) Levulinic acid biorefineries: new challenges for efficient utilization of biomass. *ChemSusChem* 9(6):562–582
- Riechert O, Husham M, Sadowski G, Zeiner T (2015) Solvent effects on esterification equilibria. *AIChE J* 61(9):3000–3011
- Růžička Jr V, Domalski ES (1993) Estimation of the heat capacities of organic liquids as a function of temperature using group additivity. *J Phys Chem Ref Data* 22(3)
- Schwartz TJ, O'Neill BJ, Shanks BH, Dumesic JA (2014) Bridging the chemical and biological catalysis gap: challenges and outlooks for producing sustainable chemicals. *ACS Catal* 4(6):2060–2069
- Serrano-Ruiz JC, Luque R, Sepulveda-Escribano A (2011) Transformations of biomass-derived platform molecules: from high added-value chemicals to fuels via aqueous-phase processing. *Chem Soc Rev* 40(11):5266–5281
- Timokhin BV, Baransky VA, Eliseeva GD (1999) Levulinic acid in organic synthesis. *Russ Chem Rev* 68(1):73–84
- Turner MK (1995) Biocatalysis in organic chemistry (part II): present and future. *Trends Biotechnol* 13(7):253–258
- Verevkin SP, Emel'yanenko VN (2012) Renewable platform-chemicals and materials: thermochemical study of levulinic acid. *J Chem Thermodyn* 46:94–98
- Weingarten R, Tompsett GA, Conner WC, Huber GW (2011) Design of solid acid catalysts for aqueous-phase dehydration of carbohydrates: the role of Lewis and Brønsted acid sites. *J Catal* 279(1):174–182
- Werpy T, Petersen G (2004) Top value added chemicals from biomass: volume I—results of screening for potential candidates from sugars and synthesis gas.; National Renewable Energy Lab., Golden, CO (US), p medium: ED; size: 76 pp. pages

- Wolbach JP, Sandler SI (1998) Using molecular orbital calculations to describe the phase behavior of cross-associating mixtures. *Ind Eng Chem Res* 37(8):2917–2928
- Wu K, Wu Y, Chen Y, Chen H, Wang J, Yang M (2016) Heterogeneous catalytic conversion of biobased chemicals into liquid fuels in the aqueous phase. *ChemSusChem* 9(12):1355–1385
- Yadav GD, Borkar IV (2008) Kinetic modeling of immobilized lipase catalysis in synthesis of n-butyl levulinate. *Ind Eng Chem Res* 47(10):3358–3363
- Zhang Y-HP (2008) Reviving the carbohydrate economy via multi-product lignocellulose biorefineries. *J Ind Microbiol Biotechnol* 35(5):367–375
- Zhang J, Wu S, Li B, Zhang H (2012) Advances in the catalytic production of valuable levulinic acid derivatives. *ChemCatChem* 4(9):1230–1237